PHYSICAL REVIEW B **89**, 140404(R) (2014)

Magnetocrystalline anisotropy in x-ray magnetic linear dichroism at the 3*p* edges of crystalline Fe thin films

M. F. Tesch,[1,*] D. Legut,[2] H.-Ch. Mertins,[1] M. C. Gilbert,[1] C. Jansing,[1] J. Hamrle,[2] J. Rusz,[3] P. M. Oppeneer,[3] D. E. Bürgler,[4] C. M. Schneider,[4,5] A. Gaupp,[6] and U. Berges[7]

[1]*University of Applied Sciences Münster, Stegerwaldstraße 39, D-48565 Steinfurt, Germany*

[2]*VSB - Technical University of Ostrava, 17. Listopadu 15, CZ-70833 Ostrava, Czech Republic*

[3]*Department of Physics and Astronomy, Uppsala University, P. O. Box 516, S-751 20 Uppsala, Sweden*

[4]*Peter Grünberg Institut (PGI-6) and Jülich-Aachen Research Alliance (JARA-FIT), Forschungszentrum Jülich GmbH, D-52425 Jülich, Germany*

[5]*Fakultät für Physik and Center for Nanointegration Duisburg-Essen (CeNIDE), Universität Duisburg-Essen, D-47048 Duisburg, Germany*

[6]*Helmholtz Zentrum Berlin, Albert-Einstein-Straße 15, D-12489 Berlin, Germany*

[7]*DELTA, Maria-Goeppert-Mayer-Straße 2, D-44227 Dortmund, Germany*

(Received 13 November 2013; published 14 April 2014)

X-ray magnetic linear dichroism spectra measured in reflection (XMLD-R) on crystalline bcc Fe thin films across the 3*p* absorption edges are reported. A series of measurements with varying orientation of the electric field vector of the linear polarized synchrotron radiation with respect to the crystal axes reveals a strong magnetocrystalline anisotropy in the XMLD-R spectra. The spectra agree well with theoretical spectra calculated within the framework of the density-functional theory accounting for the spin-orbital and exchange splitting of the 3*p* semicore states on an equal footing.

DOI: 10.1103/PhysRevB.89.140404 PACS number(s): 75.30.Gw, 78.20.Ls, 78.70.Ck

X-ray magnetic circular dichroism (XMCD) and the transversal magneto-optical Kerr effect (T-MOKE) are powerful tools to investigate ferromagnetic materials, as these magnetic spectroscopies probe a material's optical response that is linear in the magnetization [1]. In contrast, the x-ray magnetic linear dichroism (XMLD) [1,2] measured in transmission or absorption is suited to investigate antiferromagnetic (AFM) materials [3] because it probes the response which is quadratic in the magnetization. Moreover, XMLD spectroscopy is very sensitive to the crystallographic orientation of the magnetization direction [4], much more than the XMCD or T-MOKE [1,5]. Large XMLD anisotropy signals for 3*d* atoms in cubic crystal fields have been predicted [4] and were observed in the past few years at the 2*p* core levels of 3*d* elements [6–8]. Recently it was proposed that the sensitivity of XMLD spectroscopy at the 2*p* edges could even be employed to distinguish between competing models of electronic band structures [9,10].

In contrast to the 2*p* edges, investigations of the XMLD at the 3*p* semicore levels of 3*d* metals are lacking. These shallow core levels have recently gained considerable importance. Through the development of novel x-ray sources, such as free-electron lasers and table-top high-harmonic generation (HHG) sources, capable of delivering brilliant radiation in the XUV regime, the 3*p* (*M*) edges have come into the focus of magnetism research [11–15]. Very recently, using radiation from a HHG source, T-MOKE at the 3*p* edges has been exploited to study the ultrafast magnetization dynamics response of permalloy in an element-selective way at the Fe and Ni 3*p* edges [13,14,16]. Magnetic x-ray scattering of XUV from a free-electron laser was used to study the femtosecond dynamical magnetic response of a Co/Pt multilayer at the Co 3*p* edge [15]. These recent studies request a deep understanding of the magnetic spectroscopy of 3*p* edges, but to date only a few XMCD and T-MOKE studies have been performed [17–19], and only one XMLD study was reported [20]. In particular, an understanding of how the measured spectra relate to quantities giving rise to atomic magnetism, i.e., the exchange and spin-orbit interactions, has not yet been achieved. Approximations in the theoretical description that are valid at the 2*p* levels, which exhibit a large spin-orbit splitting but tiny exchange splitting, do not hold any longer at the 3*p* edges where these quantities are of similar magnitude (1–2 eV) [20].

Here we report a combined experimental and theoretical investigation of the 3*p*-edge XMLD spectra of crystalline Fe thin films, measured in reflection, and particularly, of the magnetocrystalline anisotropy present in the dichroic signal.

Background. Conventional XMLD spectroscopy using electron yield techniques can suffer from the influence of the applied magnetic field on the detected signal, but photon-in–photon-out reflectivity measurements are not disturbed. Also, because of the low absorption at the 3*p* edges, it is advantageous to measure the XMLD in reflection (XMLD-R). XMLD-R spectroscopy has been previously applied to study buried AFM layers [21].

The XMLD-R signal is experimentally deduced from the difference of two reflection spectra measured in the geometry sketched in Fig. 1. The first reflection spectrum $R(H_{\parallel})$ is taken with magnetic field $H_{\parallel}$ parallel to the electric field vector E of the incoming linearly polarized light (Fig. 1). The second reflection spectrum $R(H_{\perp})$ is obtained for a magnetic field $H_{\perp}$ perpendicular to the electric field vector. The magnitude of the magnetic field ensures that the sample magnetization always points along the external field.

The XMLD-R can be defined in two alternative ways. First, through the difference spectrum $\Delta R = R(H_{\parallel}) - R(H_{\perp})$,

*marc.tesch@fh-muenster.de

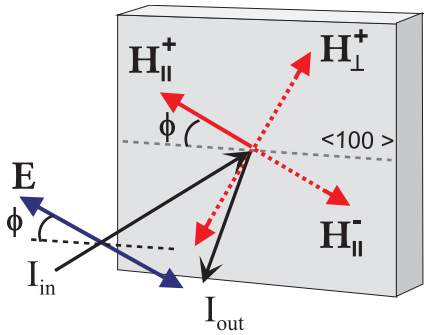

FIG. 1. (Color online) Experimental geometry for the detection of XMLD-R spectra. The reflectivity $R = I_{out}/I_{in}$ is measured on a crystalline sample for four relative orientations of polarization E and saturating field H and at variable angle ϕ, which is defined with respect to a crystal axis, e.g., $\langle 100 \rangle$. Note that in practice only one, but a rotatable, magnetic field is applied, e.g., $H_{\parallel}^{+}$.

which contains the fundamental dichroic signal. Second, ΔR may be normalized to the sum $2\overline{R} = R(H_{\parallel}) + R(H_{\perp})$ according to $A = \Delta R/2\overline{R}$ to obtain the relative amount, i.e., the XMLD-R asymmetry, of the dichroism. Both ΔR and A measure a magneto-optical effect that is to lowest order quadratic in the magnetization [21]. To avoid unintended enhancement of the asymmetry A due to interference effects stemming from multiple reflections or due to small reflectivity in some spectral range we use in the following the difference ΔR. Furthermore, for ferromagnetic materials there may appear additional terms in A and ΔR which are linear in the magnetization when the measurement is not precisely at normal incidence (as is the case in our setup). To avoid these contributions we measured the reflection spectra $R(H_{\parallel,\perp})$ each for two antiparallel magnetization directions $H_{\parallel,\perp}^{+}$ and $H_{\parallel,\perp}^{-}$ and replaced $R(H_{\parallel,\perp})$ by $R(H_{\parallel,\perp}) = [R(H_{\parallel,\perp}^{+}) + R(H_{\parallel,\perp}^{-})]/2$, leading to

$$\Delta R = [R(H_{\parallel}^{+}) + R(H_{\parallel}^{-}) - R(H_{\perp}^{+}) - R(H_{\perp}^{-})]/2. \qquad (1)$$

The detection of the magnetocrystalline anisotropy of ΔR is performed by scanning the angle ϕ between a certain crystalline axis (e.g., the $\langle 100 \rangle$ axis) and the electric field vector E (Fig. 1).

Experiment. The room temperature experiments were performed at the undulator beamline U125-2-SGM2 of BESSY [22]. The spectral resolution across the $3p$ edges near 60 eV was $E/\Delta E = 3000$. The incident light was linearly p polarized with a polarization degree above 0.99. The spectra were measured with the BESSY ultrahigh vacuum polarimeter chamber [23]. *In situ* exchange and removal of samples allowed for quasisimultaneous detection of the incident and reflected light in order to measure the absolute reflectance using a GaAs:P diode. The reflection spectra were taken by monitoring the reflected intensity at each fixed photon energy for the magnetization directions $H_{\parallel}^{+}$, $H_{\perp}^{+}$, $H_{\parallel}^{-}$, and $H_{\perp}^{-}$ (see Fig. 1). From these the XMLD-R spectra were obtained according to Eq. (1). The magnetic field with fixed strength of 220 mT was created by eight permanent NdFeB magnets mounted on a rotatable ring, providing a homogeneous dipole field in the sample area. This allowed us to set any angle of the in-plane magnetization with respect to the crystal axes and/or to the electric field vector. The XMLD reflection spectra were taken in near-normal incidence at $\theta = 85^{\circ}$ with respect to the sample surface.

We investigated epitaxial films of 30 and 50 nm Fe, each grown by molecular beam epitaxy on a Ag(001) buffer layer deposited on a 7 mm × 7 mm large GaAs(001) wafer using a Fe nucleation layer [24]. A 3 nm Au layer prevents oxidation. The samples were mounted such that $\phi = 0^{\circ}$ means E field parallel to the sample edge, i.e., parallel to an Ag$\langle 110 \rangle$ direction. Fe is well known to grow on Ag(001) in the bcc structure with the Fe$\langle 100 \rangle$ axis aligned with the Ag$\langle 110 \rangle$ direction [25]. This growth mode was confirmed for our Fe films by *in situ* low-energy electron diffraction (LEED). Hence, for the Fe films $\phi = 0^{\circ}$ means that the E field of the light is parallel to the $\langle 100 \rangle$ axis, which is a magnetic easy in-plane axis of Fe(001) films.

Computational modeling. The electronic structure of bulk bcc Fe was calculated with the WIEN2K code [26] using the local spin density approximation (LSDA) [27] for the exchange-correlation term and including the spin-orbit interaction. Details of the calculations are given in Ref. [28]. The absorptive permittivity tensor elements $\epsilon_{ij}(\omega)$ were computed from the linear response expressions [29], after which the full complex permittivity tensor was obtained by Kramers-Kronig transformation.

A comparison of experimental and *ab initio* computed data revealed discrepancies in the reflectivity in the nonresonant energy range. While the experiment shows a smoothly decaying reflectivity in the pre- and post-edge energy region, the calculated reflectivity almost reaches zero. This indicates that an additional optical background absorption needs to be included in the calculations to compensate the underestimated reflectivity in the nonresonant energy regions. In the measured photon energy range we described the background absorption by a simple model (including only diagonal elements): $\mathrm{Im}[\varepsilon_{ii}^{\mathrm{back}}] = A\exp(-E/E_{\mathrm{dec}})$, for which we found an amplitude $A = 0.4$ and a decay energy $E_{\mathrm{dec}} = 40$ eV; $\mathrm{Re}[\varepsilon_{ii}^{\mathrm{back}}]$ was determined by Kramers-Kronig transformation. Furthermore, the full optics of the multilayer structure was described by an in-house optical program for solving the light propagation in the multilayered structure (air/Au/metal/Ag/air) [30]. The sample roughness was accounted for by a scalar diffraction theory [31,32], where sample roughness $\sigma = 3$ nm and correlation length $T = 10$ nm were used. Note that the inclusion of sample roughness is important, since for the examined samples it was measured to be about 1–3 nm and therefore it is not negligible compared to the wavelength of the incident light. The roughness model concerns the first interface, i.e., between air and the capping Au layer, as the change of the reflectivity is higher than for the Au/metal interface. The output of the light propagation simulation is a reflection matrix of the whole multilayered structure, for an arbitrary magnetization orientation. It allows us to calculate the XMLD-R in a way analogous to the measurement.

Results. XMCD hysteresis curves (not shown) were measured in reflection on the Fe films at beamline 12 at the synchrotron facility DELTA (Dortmund, Germany) using the polarimeter chamber XMAPS [33]. These data confirm that for the 50 nm bcc Fe film the medium hard axis is along $\langle 110 \rangle$, $\phi = 45^{\circ}$ with a saturation field of $B \approx 80$ mT, and the easy axis is along $\langle 100 \rangle$, $\phi = 0^{\circ}$ with a saturation field of $B \approx 3$ mT, as

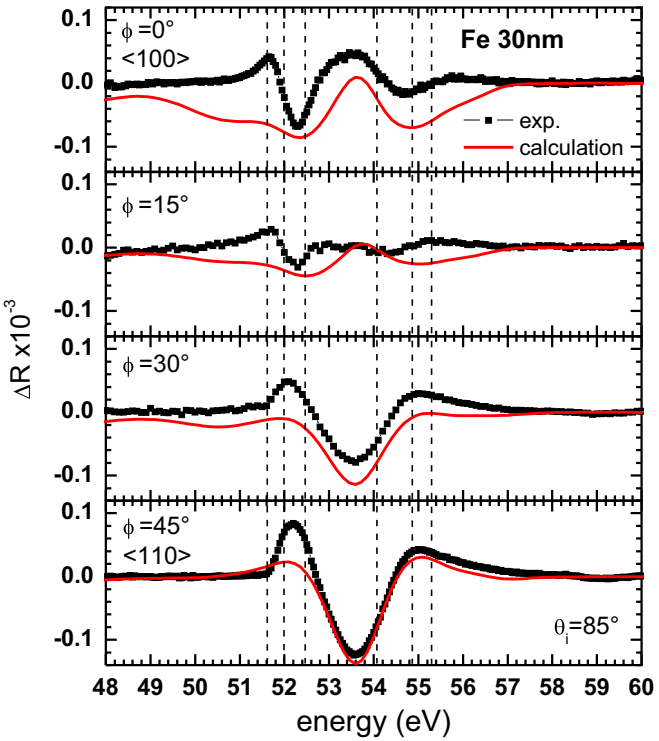

FIG. 2. (Color online) XMLD-reflection spectra (ΔR) measured across the $3p$ edge of a 30 nm bcc Fe film at near-normal incidence $\theta = 85^\circ$ for different orientations ϕ of the E field with respect to the $\langle 100 \rangle$ crystal axis. The experimental results are given by the black points, the result of *ab initio* calculations by the full curves. The vertical lines denote the positions of the computed single j_z levels of the $3p_{3/2}$ and $3p_{1/2}$ states.

expected from the bulk properties. Note that the applied field was sufficient to saturate the samples.

To investigate the magnetic anisotropy of the XMLD, a series of XMLD-R spectra have been measured on the Fe sample for $\theta = 85^\circ$ and for a set of angles ϕ between the electric field vector and the crystalline axes of the sample (see Fig. 1).

The measured XMLD-R spectra are shown in Fig. 2, together with *ab initio* computed spectra. A strong and clearly discernible dependence on the direction of the E field with respect to the magnetic easy and medium-hard axis (angle ϕ) is observed.

Notably, the XMLD-R structures for the medium-hard axis ($\phi = 45^\circ$) are inverted with respect to those of the easy axis ($\phi = 0^\circ$) and changes in the peak height of up to 100% are observed. Such strong magnetocrystalline anisotropy of XMLD has been detected for XMLD spectra taken at the $2p$ edge [6–8]. Here this property is to our knowledge observed for the first time at the $3p$ edge. The normalized asymmetry $A = \Delta R/2\overline{R}$ reaches peak values of 0.7%, which is a factor of 2 smaller than those obtained at the $2p$ edge [8].

The trends of the *ab initio* calculated XMLD-R spectra are in good agreement with the measured spectra. A nearly perfect agreement is found when the electric field is aligned with the $\langle 110 \rangle$ axis, while there are some deviations for the $\langle 100 \rangle$ orientation of E at the low energy side of the $3p$ resonance. The good correspondence indicates that relativistic *ab initio* calculations provide an adequate description of the semicore $3p$ states, exhibiting a spin-orbit and an exchange splitting of similar size (1–2 eV), which leads to hybridization of the individual j_z states of the $3p_{1/2}$ and $3p_{3/2}$ levels [20]. The positions of these **k**-wave vector dependent $3p$ states are marked in Fig. 2 as vertical lines. The levels indicate the initial states for the optical transitions into the valence band and cover the full energy range of the XMLD structures.

In addition, the measured magnetocrystalline anisotropy in the XMLD-R spectra is relatively well described. This property arises from the crystal-field split, spin-polarized e_g and t_{2g} $3d$-valence states, being selectively probed by optical transitions from the semicore states [4]. (Note that the computed XMLD-R spectra were multiplied by 80 because the *ab initio* calculations underestimated the reflectivity of the Fe sample.) This, however, might be, for example, due to interference effects or due to an underestimated background in the measurements. The edge energy has been shifted by 1 eV to align with the measured edge position and to account for the resolution of the measurement we applied a constant 2 eV Lorentzian broadening over the whole energy range.

A very comprehensive demonstration of the magnetocrystalline anisotropy in XMLD-R of the Fe sample is obtained through a polar plot, presented in Fig. 3. The photon energy was fixed at 52.25 eV where a maximum dependence of the XMLD-R signal as function of the angle ϕ is present (see Fig. 2). The angle ϕ was moved in steps of 7.5° from $\phi = 0^\circ$ to 360°. The angular plot reveals a nearly perfect fourfold magnetic anisotropy. A maximum, positive XMLD-R signal is obtained for the equivalent angles $\phi = 45^\circ$, 135°, 225°, and 315° [in-plane hard axes of Fe(001)], whereas negative XMLD-R signals with values below the dashed zero line are obtained for $\phi = 0^\circ$ and equivalent angles [in-plane easy axes of Fe(001)]. The fourfold symmetry unambiguously demonstrates the crystalline quality of the sample and the well-defined relation between the XMLD-R anisotropy and the

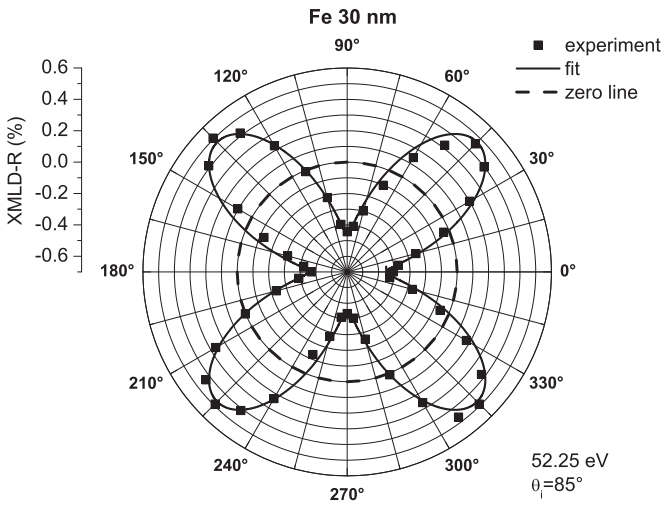

FIG. 3. Polar plot of the XMLD-R asymmetry A measured on a 30 nm Fe film at 52.25 eV; $\phi = 0^\circ$ corresponds to the Fe $\langle 100 \rangle$ easy axis. The full line shows an ideal sinusoidal curve with fourfold symmetry.

in-plane magnetocrystalline anisotropy energy of the film. This observation reflects the common origin of magnetocrystalline anisotropy energy and the anisotropy of the XMLD-R signal, which both are manifestations of the effect of spin-orbit coupling on the band structure.

Concluding. Our experiments of the XMLD at the $3p$ edges of Fe reveal the existence of appreciable changes in the XMLD-R spectra, related to the magnetocrystalline anisotropy. These XMLD anisotropies measured in reflection are similarly large as those previously detected at the $2p$ edges in absorption (cf. Refs. [6–8]). We find that the XMLD-R spectra of the Fe film and their magnetic anisotropy are well described by *ab initio* calculations based on the effective single-electron approach of the density-functional theory. The high sensitivity of XMLD to the orientation of the magnetization in the local crystal field opens possibilities for employing the $3p$ edges for illuminating investigations of static magnetism as well as dynamical magnetic processes in transition-metal compounds and alloys.

Acknowledgments. This work has been supported through the Swedish Research Council (VR) and the Swedish National Infrastructure for Computing (SNIC). D.L. and J.H. acknowledge partial financial supported by the Grant Agency of the Czech Republic, Project No. 13-30397S. D.L., M.T., and H.-Ch.M. acknowledges also the Mobility Grant 7AMB13DE004. D.L. acknowledges partial computational support within the IT4Innovations Centre (CZ.1.05/1.1.00/02.0070). M.T., H.-Ch.M., M.G., and C.J. thankfully acknowledge the financial support from HZB.

[1] J. Stöhr and H. C. Siegmann, *Magnetism—From Fundamentals to Nanoscale Dynamics* (Springer, Berlin, 2006).

[2] J. B. Kortright and S.-K. Kim, Phys. Rev. B **62**, 12216 (2000).

[3] F. Nolting, A. Scholl, J. Stöhr, J. W. Seo, J. Fompeyrine, H. Siegwart, J.-P. Locquet, S. Anders, J. Lüning, E. E. Fullerton, M. F. Toney, M. R. Scheinfein, and H. A. Padmore, Nature (London) **405**, 767 (2000).

[4] J. Kuneš and P. M. Oppeneer, Phys. Rev. B **67**, 024431 (2003).

[5] A. Kleibert, V. Senz, J. Bansmann, and P. M. Oppeneer, Phys. Rev. B **72**, 144404 (2005).

[6] E. Arenholz, G. van der Laan, R. V. Chopdekar, and Y. Suzuki, Phys. Rev. Lett. **98**, 197201 (2007).

[7] G. van der Laan, E. Arenholz, R. V. Chopdekar, and Y. Suzuki, Phys. Rev. B **77**, 064407 (2008).

[8] F. Nolting, D. Legut, J. Rusz, P. M. Oppeneer, G. Woltersdorf, and C. H. Back, Phys. Rev. B **82**, 184415 (2010).

[9] M. Kallmayer, P. Klaer, H. Schneider, G. Jakob, H. J. Elmers, D. Legut, and P. M. Oppeneer, Phys. Rev. B **84**, 054448 (2011).

[10] M. Meinert, J.-M. Schmalhorst, M. Glas, G. Reiss, E. Arenholz, T. Böhnert, and K. Nielsch, Phys. Rev. B **86**, 054420 (2012).

[11] C. Gutt, S. Streit-Nierobisch, L.-M. Stadler, B. Pfau, C. M. Günther, R. Könnecke, R. Frömter, A. Kobs, D. Stickler, H. P. Oepen, R. R. Fäustlin, R. Treusch, J. Feldhaus, E. Weckert, I. A. Vartanyants, M. Grunze, A. Rosenhahn, T. Wilhein, S. Eisebitt, and G. Grübel, Phys. Rev. B **81**, 100401 (2010).

[12] B. Vodungbo, J. Gautier, G. Lambert, A. Barszczak-Sardinha, M. Lozano, S. Sebban, M. Ducousso, W. Boutu, K. Li, B. Tudu, M. Tortarolo, R. Hawaldar, R. Delaunay, V. López-Flores, J. Arabski, C. Boeglin, H. Merdji, P. Zeitoun, and J. Lüning, Nat. Commun. **3**, 999 (2012).

[13] S. Mathias, C. La-O-Vorakiat, P. Grychtol, P. Granitzka, E. Turgut, J. M. Shaw, R. Adam, H. T. Nembach, M. E. Siemens, S. Eich, C. M. Schneider, T. J. Silva, M. Aeschlimann, M. M. Murnane, and H. C. Kapteyn, Proc. Natl. Acad. Sci. USA **109**, 4792 (2012).

[14] D. Rudolf, C. La-O-Vorakiat, M. Battiato, R. Adam, J. M. Shaw, E. Turgut, P. Maldonado, S. Mathias, P. Grychtol, H. T. Nembach, T. J. Silva, M. Aeschlimann, H. C. Kapteyn, M. M. Murnane, C. M. Schneider, and P. M. Oppeneer, Nat. Commun. **3**, 1037 (2012).

[15] B. Pfau, S. Schaffert, L. Müller, C. Gutt, A. Al-Shemmary, F. Büttner, R. Delaunay, S. Düsterer, S. Flewett, R. Frömter, J. Geilhufe, E. Guehrs, C. M. Günther, R. Hawaldar, M. Hille, N. Jaouen, A. Kobs, K. Li, J. Mohanty, H. Redlin, W. F. Schlotter, D. Stickler, R. Treusch, B. Vodungbo, M. Kläui, H. P. Oepen, J. Lüning, G. Grübel, and S. Eisebitt, Nat. Commun. **3**, 1100 (2012).

[16] C. La-O-Vorakiat, M. Siemens, M. M. Murnane, H. C. Kapteyn, S. Mathias, M. Aeschlimann, P. Grychtol, R. Adam, C. M. Schneider, J. M. Shaw, H. Nembach, and T. J. Silva, Phys. Rev. Lett. **103**, 257402 (2009).

[17] H. Höchst, D. Rioux, D. Zhao, and D. L. Huber, Phys. Rev. B **65**, 064439 (2002).

[18] M. Hecker, P. M. Oppeneer, S. Valencia, H.-C. Mertins, and C. M. Schneider, J. Elect. Spectrosc. Relat. Phenom. **144–147**, 881 (2005).

[19] S. Valencia, A. Gaupp, W. Gudat, H.-C. Mertins, P. M. Oppeneer, D. Abramsohn, and C. M. Schneider, New J. Phys. **8**, 254 (2006).

[20] S. Valencia, A. Kleibert, A. Gaupp, J. Rusz, D. Legut, J. Bansmann, W. Gudat, and P. M. Oppeneer, Phys. Rev. Lett. **104**, 187401 (2010).

[21] P. M. Oppeneer, H.-C. Mertins, D. Abramsohn, A. Gaupp, W. Gudat, J. Kuneš, and C. M. Schneider, Phys. Rev. B **67**, 052401 (2003).

[22] M. Martins, G. Kaindl, and N. Schwentner, J. Elec. Spectrosc. Relat. Phenom. **101–103**, 965 (1999).

[23] F. Schäfers, H.-C. Mertins, A. Gaupp, W. Gudat, M. Mertin, I. Packe, F. Schmolla, S. D. Fonzo, G. Soullié, W. Jark, R. Walker, X. L. Cann, R. Nyholm, and M. Eriksson, Appl. Opt. **38**, 4074 (1999).

[24] D. E. Bürgler, C. M. Schmidt, J. A. Wolf, T. M. Schaub, and H.-J. Güntherodt, Surf. Sci. **366**, 295 (1996).

[25] D. E. Bürgler, C. M. Schmidt, D. M. Schaller, F. Meisinger, R. Hofer, and H.-J. Güntherodt, Phys. Rev. B **56**, 4149 (1997).

[26] P. Blaha, K. Schwarz, G. K. H. Madsen, D. Kvasnicka, and J. Luitz, An Augmented Plane Wave + Local Orbitals Program for Calculating Crystal Properties, Techn. Univ. Wien, Austria (2001).

[27] J. P. Perdew and Y. Wang, Phys. Rev. B **45**, 13244 (1992).

[28] The energy cutoff expressed as product of the muffin-tin radius R_{MT} and the maximum reciprocal space vector K_{max} was 8.5, the largest reciprocal vector in the charge Fourier expansion G_{max} was set to 14 $Ry^{1/2}$, and the maximum value of partial waves inside muffin-tin spheres l_{max} was 10. A grid of $27\times27\times27$ k points was used to sample the first Brillouin zone. A finer k-point mesh of $81\times81\times81$ was used to determine optical transition matrix elements among all bands and k-wave vectors .

[29] C. Ambrosch-Draxl and J. O. Sofo, Comput. Phys. Commun. **175**, 1 (2006).

[30] S. Višňovský, Czech. J. Phys. **41**, 663 (1991).

[31] K. Postava, H. Sueki, M. Aoyama, T. Yamaguchi, K. Murakami, and Y. Igasaki, Appl. Surf. Sci. **175**, 543 (2001).

[32] I. Ohlídal and F. Lukeš, Opt. Acta **19**, 817 (1972).

[33] M. F. Tesch, M. C. Gilbert, H.-C. Mertins, D. E. Bürgler, U. Berges, and C. M. Schneider, Appl. Opt. **52**, 4294 (2013).